Effect of *N,N′*-bis(benzoic) 1,4-cyclohexanedicarboxylic acid dihydrazide on poly(L-lactide) crystallization

Yang Lv[1], Ninghui Tan[1), *)], Hui Zhang[1], Yanhua Cai[1), *)] (ORCID ID: 0000-0002-1390-3722), **Xiaoqin Zhou[2]**

DOI: https://doi.org/10.14314/polimery.2025.6.5

Abstract: Effect of *N,N′*-bis(benzoic) 1,4-cyclohexanedicarboxylic acid dihydrazide (CADBH) on the crystallization of poly(L-lactide) (PLLA) was investigated. CADBH (0.4–3 wt%) was introduced into PLLA by melt mixing. DSC confirmed that PLLA crystallization depends on both CADBH content and cooling and heating rates. The minimum crystallization half-life (35.4 s) was obtained at 115°C with 3 wt% CADBH. However, a small addition of CADBH had an unfavorable effect on PLLA transparency.

Keywords: PLLA, benzoic hydrazide, crystallization, transparency.

Wpływ dihydrazydu kwasu *N,N′*-bis(benzoilo) 1,4-cykloheksanodikarboksylowego na krystalizację poli(L-laktydu)

Streszczenie: Zbadano wpływ dihydrazydu kwasu *N,N′*-bis(benzoilo) 1,4-cykloheksanodikarboksylowego (CADBH) na krystalizację poli(L-laktydu) (PLLA). CADBH (0,4–3 % mas) wprowadzano do PLLA w procesie mieszania w stopie. Metodą DSC potwierdzono, że krystalizacja PLLA zależy zarówno od zawartości CADBH, jak i szybkości chłodzenia i ogrzewania. Minimalny półokres krystalizacji (35,4 s) uzyskano w temperaturze 115°C przy zawartości 3% mas. CADBH. Jednak niewielki dodatek CADBH miał niekorzystny wpływ na przezroczystość PLLA.

Słowa kluczowe: PLLA, hydrazyd benzoesowy, krystalizacja, przezroczystość.

Plastic is an indispensable material in the modern world thanks to its own advantages in terms of low density, high performance, low manufacturing cost, wide functionalities, etc. However, most plastics are produced from petroleum, resulting in their non-degradation and serious environmental pollution after usage. Thus, using bio-based plastic is highly desirable to alleviate energy crises and promote green economic development. Poly(L-lactide) (PLLA) as the frontrunner in biopolymers possesses its advantages such as low carbon footprint, good processability, excellent mechanical properties, good optical transparency and more ecofriendly profile compared to other biopolymers [1–3], and these significant merits are accelerating PLLA's commercial application in fast food boxes, shopping bags, agricultural film, biomedicine, tissue engineering and 3D printing consumables [4-10], for example, PLLA was combined with Osage orange wood to prepare a polymer composite as an agricultural film, the related measurement showed that PLLA composite containing Osage orange wood exhibited the advantage of being fully biodegradable over a single growing season, and the mechanical properties of PLLA composite containing Osage orange wood could be comparable to the current agricultural mulch film [11].

PLLA as a semi-crystalline polyester possesses a relative high melting temperature about 170°C, but some shortcomings, like low crystallinity after injection molding, slow crystallization rate and poor heat resistance [12], exhibit an inhibition for PLLA's wider utilization, among these drawbacks, slow crystallization rate is a determining factor of affect PLLA's performances, especially crystallinity and heat resistance. What is worse, improving PLLA's crystallization rate through varying contents of L- and D-lactic acid during synthesis stage is difficulty, thus, introducing a nucleating agent in PLLA resin is thought to be an economical, simple and efficient method to accelerate PLLA's crystallization rate *via* reducing the free energy barrier for the formation of a critical nucleus and increasing nucleation sites [12–14]. Nowadays, nucleating agents for PLLA are classified into inorganic and organic types based on their molecular structures, and among these nucleating agents, the most popular nucleating agents include talc [15], metals phenylphosphonate [16, 17], nano inorganic salts [18, 19], amide compounds [20], TMC series compounds [21–23], etc.

Although some nucleating agents like talc and TMC have been commercially developed to enhance PLLA's

---

[1] Chongqing University of Arts and Sciences, Chongqing 402160, P.R. China.

[2] Bishan Hospital of Chongqing Medical University, Chongqing 402760, P.R. China.

[*] Authors for correspondence:
278895598@qq.com, mci651@163.com

crystallization during the manufacturing of PLLA products, the nucleation ability of the existing nucleator for PLLA and category as well as quantity still exist a significant gap compared to nucleating agents for typical general plastics of PE and PP, even worse, the heat and depth of academic study on PLLA's nucleating agent have slowed down after the outbreak of novel coronavirus, and only a small amount of organic nucleating agent with novel structure had been reported. To expand the quantity of organic nucleating agents with different molecular structures and further understand the structure-activity relationship between nucleation capacity and rigid structures such as benzene and cycloalkyl.

In this work, *N, N'*-bis(benzoic) 1,4-cyclohexanedicarboxylic acid dihydrazide (CADBH) was obtained and used as a nucleating agent for PLLA. The non-isothermal melt crystallization, non-isothermal cold crystallization, isothermal crystallization, melting behavior and optical properties of PLLA/CADBH were investigated by differential scanning calorimetry (DSC), polarizing optical microscopy (POM) and light transmittance.

EXPERIMENTAL PART

Materials

1,4-cyclohexanedicarboxylic acid, benzoic acid hydrazide, *N, N*-dimethylformamide, thionyl chloride, and pyridine were purchased from Chongqing Huawei Chemical Company (Chaina). All chemicals were of analytical grade and used without further purification. PLLA was manufactured by Nature Works LLC (Blair, Nebraska, USA) with commercial grade 4032D.

Preparation of PLLA/CADBH

The synthesis of CADBH was performed according to the procedure published elsewhere [24] and is schematically shown in Fig. 1. 10 g of 1,4-cyclohexanedicarboxylic acid, 70 mL of thionyl chloride, and 1 mL of *N,N*-dimethylformamide were mixed in a 250 ml three-necked flask and heated to 80°C for 36 h with stirring, and the resulting cyclohexyl-1,4-dicarboxyl chloride was obtained by vacuum distillation. Afterwards, 0.04 mol benzoic acid hydrazide, 70 mL *N,N*-dimethylformamide and 2 mL pyridine were mixed using ultrasonic technology in 250 mL three-necked flask to ensure that the benzoic acid hydrazide was dissolved in *N,N*-dimethylformamide, and then 0.02 mol cyclohexyl-1,4-dicarboxylchloride was instantaneously incorporated into the above-mentioned mixed solution. The reaction was performed at room temperature for 1 h and 70°C for 2.5 h. The reaction mixture was transferred into water to obtain white CADBH *via* filtration and vacuum dry. Basic spectroscopic characteristics are: FT-IR (KBr) υ: 3206.8, 2944.2, 2861.8, 1653.5, 1599.2, 1577.7, 1522.8, 1497.7, 1472.8, 1395.5, 1247.2, 1212.3, 1151.5, 1078.3, 1021.1, 955.7 cm^{-1}; ^{1}H NMR (400 Hz) δ: ppm; 10.30 (s, 1H, NH), 9.84 (s, 1H, NH), 7.48~7.89 (m, 5H, Ar), 2.27 (s, H, CH), 1.87~1.89 (d, 2H, CH_2), 1.45~1.50 (t, 2H, CH_2).

Finally, PLLA containing 0.4, 0.8, 1.5, and 3 wt% CADBH were prepared by melting mixing in a counter-rotating mixer and molding method in a flat vulcanizing machine. Prior to melting mixing, PLLA and CADBH were dried to remove residual water. The melt mixing process parameters were as follows: the process temperature was 190°C, the rotor speed was 32 rpm for 7 min and 64 rpm for 7 min. Then, the PLLA/CADBH blends were subjected to hot pressing for 4 min and cold pressing for 6 min to obtain a PLLA/CADBH thin sheet.

Methods

FT-IR

FT-IR characterization of CADBH was performed using a Nicolet iS50 (ThermoFisher Scientific, Walthamm MA, USA) spectrometer with the range of 4000–400 cm^{-1}.

^{1}H NMR

^{1}H NMR characterization of CADBH was recorded on a Bruker spectrometer (Billerica, MA, USA) at 400 MHz. Prior to characterization, CADBH was dissolved in deuterium dimethyl sulfoxide.

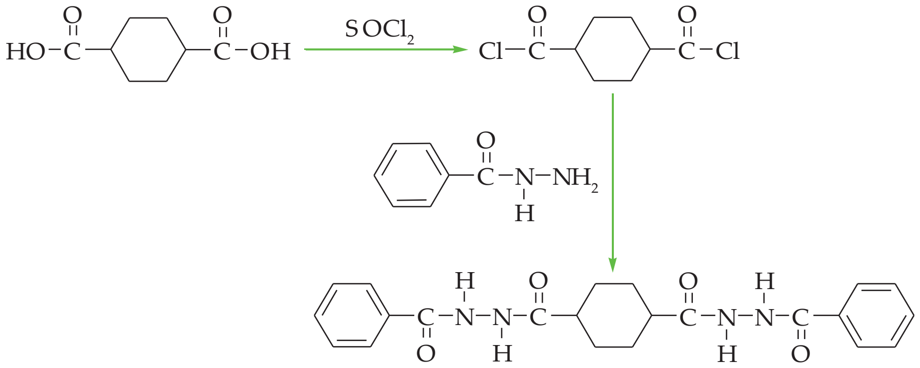

Fig. 1. CADBH synthesis scheme

DSC

The non-isothermal melt crystallization, non-isothermal cold crystallization, isothermal crystallization and melting behvaiors of PLLA/CADBH were measured by Q2000 DSC (TA Instruments, New Castle, DE, USA). Although the detailed testing conditions for non-isothermal crystallization, isothermal crystallization and melting behaviors were different, before the test, the temperature and heat flow at different rates needed to be calibrated using an indium standard. All testing samples were heated to 190°C and held at this temperature for 3 min to completely eliminate thermal history, ensuring consistent testing conditions.

Polarization optical miscroscopy (POM)

A comparative analysis of the crystalline morphology of neat PLLA and PLLA/0.4% CADBH at 115°C was performed using a DPT200ia POM (UOP, China) equipped with camera and a programmable temperature controller.

Light transmittance

The effect of CADBH and its content on light transmittance was evaluated using a DR82 light transmittance meter (Vestus Industrial Co., Huifeng, China). The light transmittance of pure PLLA and PLLA/CADBH was determined by calculating the average of five measurements.

RESULTS AND DISCUSSION

Non-isothermal melt crystallization

Investigating the non-isothermal melt crystallization behavior from the molten state was assessed, because PLLA's processing occurs mostly in the molten state as far as injecting molding is concerned. Additionally, the role of CADBH as nucleating agent also needs to be evaluated through comparing crystallization behavior of PLLA with and without CADBH. The non-isothermal melt crystallization for neat PLLA and PLLA with different CADBH loading form the molten of 190°C at a cooling rate of 1°C/min is displayed in Figure 2. As reported in the literature [25, 26], findings also indicate that the cooling process of neat PLLA hardly exhibits a non-isothermal melt crystallization peak in the DSC curve, although the cooling rate is only 1°C/min, two reasons are employed to explain this phenomenon, they are the slow homogeneous nucleation rate of PLLA itself in high-temperature region and slow crystal growth rate due to poor mobility of PLLA molecular segment in low-temperature region. In contrast, with the addition of CADBH, DSC curve presents a sharp non-isothermal melt crystallization peak, and the non-isothermal melt crystallization peak shifts toward the higher temperature side as CADBH loading increased, showing that CADBH acts as nucleating agent in cooling and effectively enhances PLLA's crystallization ability. An important role of nucleating agent is to provide the heterogeneous nucleation site in polymer resin and increase nucleation rate, resulting in that the crystallization can start at a higher temperature, which is clearly proved by the shift of non-isothermal melt crystallization peak with increasing CADBH loading. DSC thermal parameters including non-isothermal onset-crystallization temperature (T_{oc}), non-isothermal melt crystallization peak temperature (T_{mc}) and non-isothermal melt crystallization enthalpy (ΔH_c) also confirm the accelerating role of CADBH on PLLA's crystallization, as the CADBH loading increases from 0.4 wt% to 3 wt%, T_{oc} and T_{mc} increase from 139.4°C, 136.0°C to 141.5°C, 138.6°C, respectively. The difference between T_{oc} and T_{mc} decreases from 3.4°C to 2.9°C as CADBH loading increased, indicating that a higher CADBH loading is to be better for accelerating PLLA's crystallization rate, because a sharper non-isothermal melt crystallization peak often means a higher crystallization rate at the same testing level. However, it is noted that ΔH_c cannot exhibit a regular change with increasing of CADBH loading, and PLLA/0.4% CADBH has the maximum ΔH_c value 46.8 J/g.

The heating process of pure PLLA and PLLA/CADBH after non-isothermal melt crystallization was conducted to investigate the effect of CADBH on the glass transition temperature of PLLA. As can be seen from Figure 3, the T_g of pure PLLA is lower than that of PLLA/CADBH regardless of the content of crystallization agent. PLLA/CADBH formed more crystals after the non-isothermal cooling process than PLLA, which makes it much more difficult to complete the transition from the glassy state to the high-elastic state at the initial steady temperature, and this transition can only be completed at a higher temperature. Except for PLLA/0.4% CADBH, the T_g of other PLLA/CADBH is higher than 61°C, and PLLA/1.5% CADBH has a higher T_g of 62.6°C. This result is not consistent with

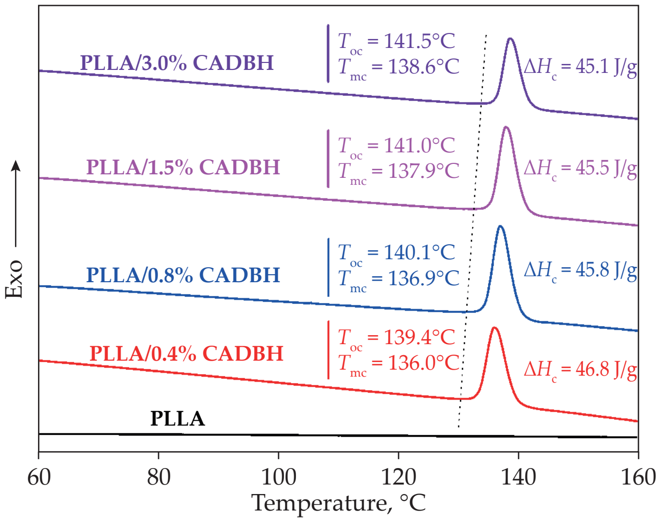

Fig. 2. DSC thermograms of neat PLLA and PLLA/CADBH at 190°C and 1°C/min heating rate

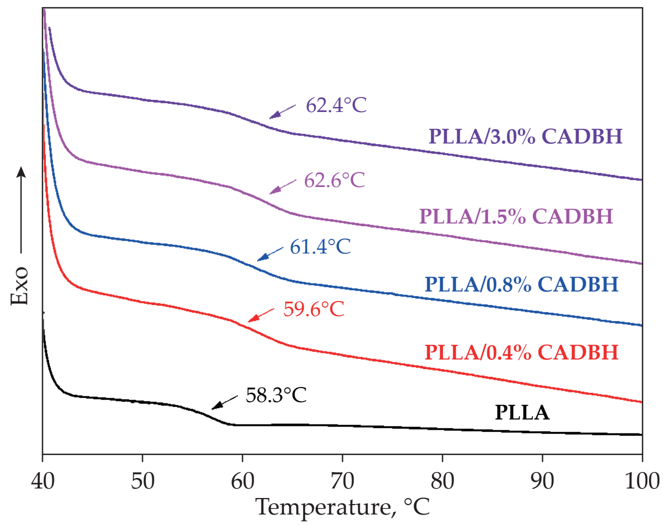

Fig. 3. T_g of neat PLLA and PLLA/CADBH at 10⚜/min heating rate, after cooling at 1°C/min

the ΔH_c after non-isothermal melt crystallization, which indicates that the T_g is not only affected by the crystallinity of PLLA but also by the content of CADBH.

For semi-crystalline polyester, manufacturers expect that rapid crystallization at a higher cooling rate will increase the yield and reduce the cost; meanwhile, at a higher cooling rate, the crystallization ability of PLLA containing a crystallizing agent can also be tested to evaluate the crystallization effect of the additive, because a higher cooling rate can shorten the crystal growth time, leading to a decrease in the crystallization ability and a reduction in the amount of crystals. As shown in Fig. 4, the effects of cooling rate on the non-isothermal crystallization behavior of PLLA/CADBH were studied by DSC. It is observed that with the increase of the cooling rate from 10°C/min to 20°C/min, the non-isothermal crystallization peak of the melt flattens and broadens, while shifting toward the low temperature. This effect is due to the decrease in the crystallization ability of PLLA/CADBH. However, all PLLA/CADBH are still able to crystallize after rapid cooling at 20°C/min, which again confirms the effect of CADBH accelerating crystallization. In addition, a higher CADBH loading can effectively prevent the decrease in crystallization ability, because at the same cooling rate, PLLA with higher CADBH content initiates crystallization at a higher temperature and shows a more pronounced non-isothermal crystallization peak of the melt.

Non-isothermal cold crystallization

Cold crystallization process was also conducted to sufficiently reveal the role of CADBH and its concentration. Figure 5 shows the DSC thermograms of PLLA with different CADBH loading from 40 to 190°C at different heating rates including 1, 2.5, 5, and 10°C/min. Two distinct regular patterns were observed. The first one shows that at a certain heating rate, the cold crystallization peak shifts toward low temperature with the increase of CADBH loading. This can be attributed to the fact that CADBH shows an inhibiting effect on the cold crystallization process of PLLA, and the maximum temperature of the cold crystallization peak of PLLA belongs to the lowest loading of CADBH. A similar regular pattern can also be found in the literature [27, 28]. Another regular pattern is that with the increase of the heating rate, the cold crystallization peak of a specific PLLA/CADBH shifts toward the high temperature and flattens, which is caused by thermal inertia. In addition, each PLLA/CADBH only shows a single melting peak during heating, and the melting peak temperature is not changed by the loading of CADBH. The only difference is that the melting peak temperature slightly shifts to the low temperature side with the increase of the heating rate, the reason is that when the heating rate becomes slower, more perfect crystals can be formed during heating, which causes the melting process to be completed only at a higher temperature.

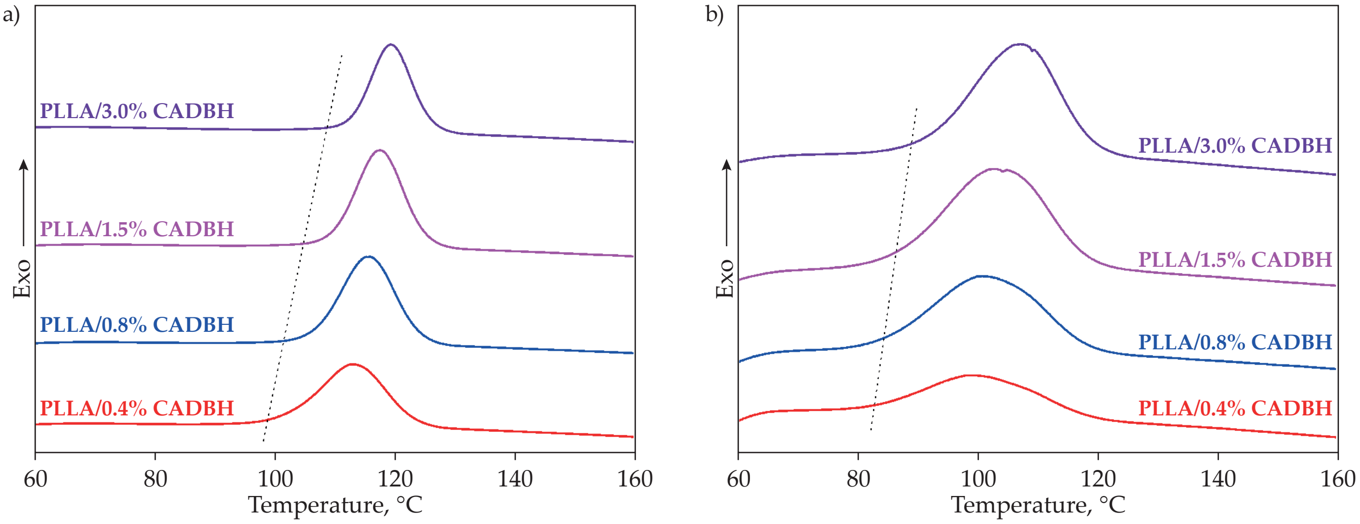

Fig. 4. Non-isothermal melt crystallization of PLLA/CADBH at 190°C and different cooling rates: a) 10°C/min, b) 20°C/min

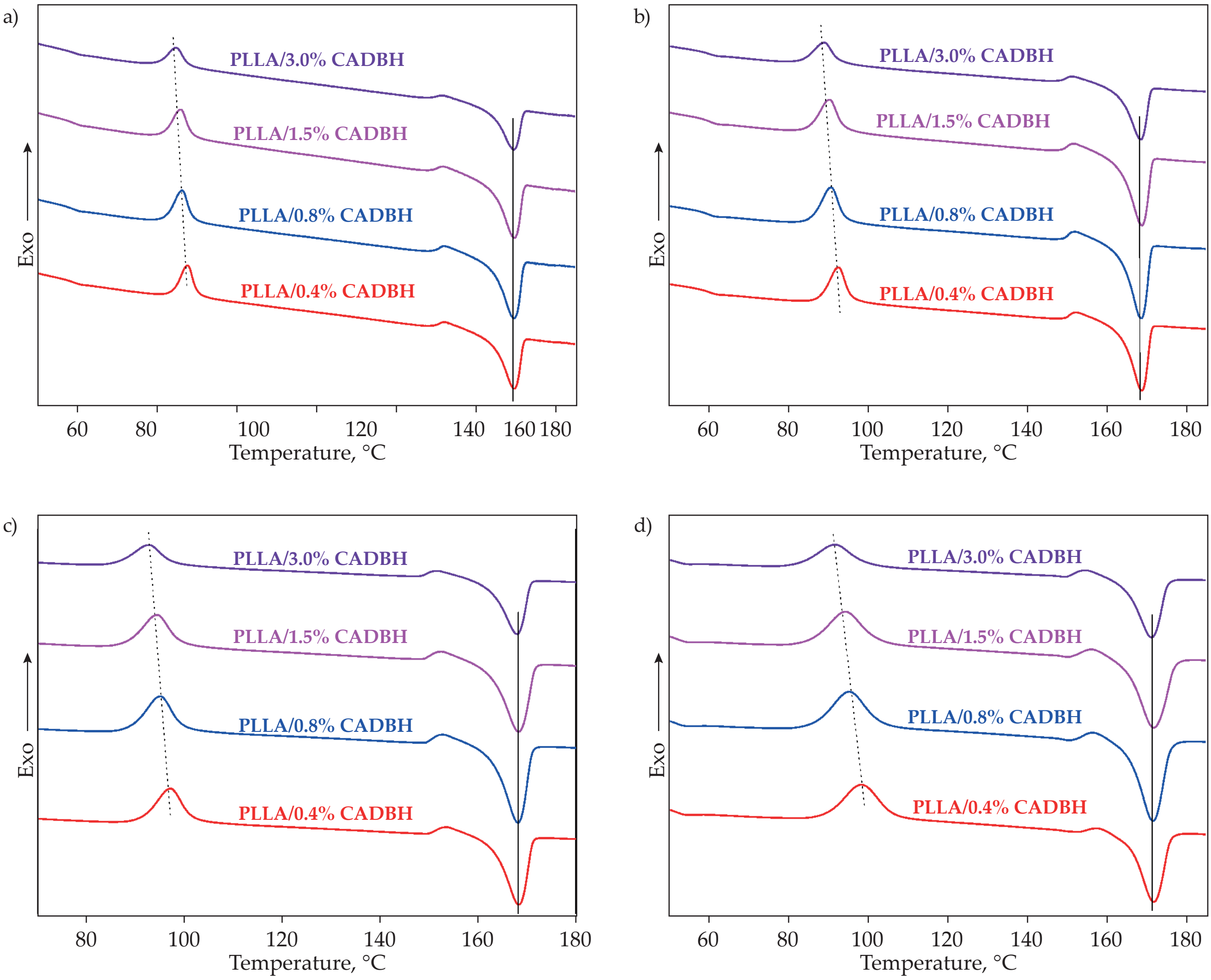

Fig. 5. DSC thermograms of PLLA/CADBH at different heating rates: a) 1°C/min, b) 2,5°C/min, c) 5°C/min, d) 10°C/min

Isothermal crystallization

Isothermal crystallization plays an important role in injection molding processes because the half time of overall crystallization $t_{1/2}$ directly determines the processing time of the related product in the mold. Therefore, the isothermal crystallization process of PLLA/CADBH at 115°C was recorded to analyze the effect of CADBH content on $t_{1/2}$ (Fig. 6). Firstly, with the increase of CADBH loading, $t_{1/2}$ decreases continuously, and PLLA/3%CADBH has the minimum $t_{1/2}$. This is because $t_{1/2}$ decreases from 58.8 to 35.4 s with the increase of CADBH loading. The isothermal crystallization enthalpy (ΔH_{ic}) also decreases from 34.1 to 29.4 J/g because the increase of crystallization rate can make the crystallization process complete faster, resulting in insufficient crystallization and the decrease of ΔH_{ic}. These results indirectly serve to corroborate the aforementioned DSC findings pertaining to non-isothermal melt crystallization, that is, PLLA/3%CADBH exhibits a more distinct non-isothermal melt crystallization peak and a shorter $t_{1/2}$, the reason is still due to the heterogeneous nucleation role of CADBH, and a larger CADBH loading can form a higher nucleation density in PLLA resin, as a result, the ability to induce crystallization of PLLA containing a higher CADBH loading significantly enhances, and the crystallization rate is significantly accelerated.

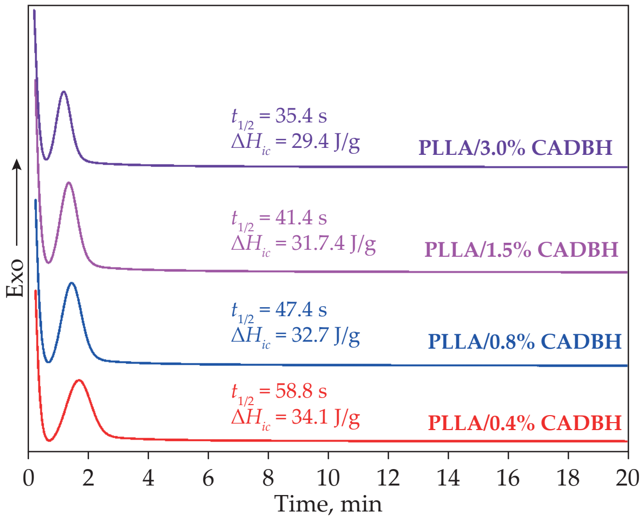

Fig. 6. Crystallization half time PLLA/CADBH at 115°C

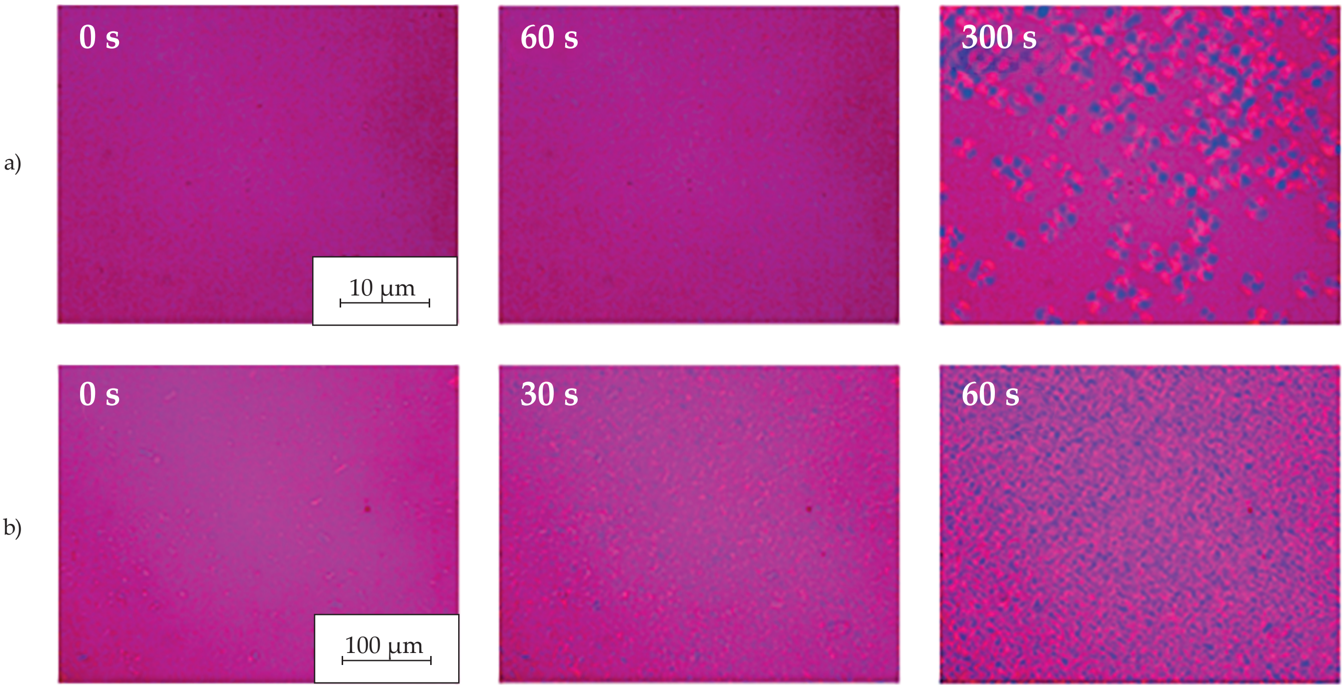

Fig. 7. POM images during isothermal crystallization at 115°C: a) neat PLLA, b) PLLA/0.4% CADBH

As mentioned earlier, CADBH is effective in accelerating the crystallization, therefore PLLA/0.4% CADBH was selected for comparison with pure PLLA to observe the crystallization process and crystal formation during isothermal crystallization at 115°C. As seen in Fig. 7, after isothermal crystallization for 60 s at 115°C, neat PLLA can display a small amount of nuclei in POM image, whereas PLLA/0.4% CADBH presents the nuclei in the beginning, and the nuclei almost pervades the entire image after isothermal crystallization for 30 s, indicating that PLLA/0.4% CADBH displays a faster nucleation speed than neat PLLA. When the isothermal crystallization time is up to 300 s, neat PLLA presents the typical spherulites structure, but the spherulites still cannot pervade the entire POM image, further suggesting PLLA's slow crystallization rate. However, in the case of PLLA/0.4% CADBH, the spherulites permeate the whole POM image after isothermal crystallization for 60 s, and the spherulite boundaries are indistinct, which is due to the mutual interaction of spherulites.

Melting behavior

To explore some physical behaviors in the melting process of PLLA/CADBH and analyze the reason of these physical behaviors, the melting processes of PLLA/CADBH after non-isothermal melt crystallization were further investigated. Fig. 8 shows PLLA/CADBH's melting processes at different heating rates corresponding to the rate of non-isothermal melt crystallization at different cooling rates (1°C/min, 2.5°C/min, and 5°C/min). It is evident that at a rate of 1°C/min, all DSC curves exhibit a single melting peak, and the melting peak temperature slightly increases from 169.3°C to 169.9°C as CADBH loading increased, but the melting enthalpy does not exhibit the regular variation, and PLLA/0.8% CADBH has the maximum melting enthalpy of 45.0 J/g. With the increase in cooling rate, the melting peak of a given PLLA/CADBH shifts toward the low-temperature side, the probable reason is that an increase in cooling rate leads to insufficient crystallization and the formation of more imperfect crystals. Additionally, when slightly increasing the rate, the double melting peaks easily appear for PLLA with low CADBH loading (0.4 wt% or 0.8 wt%), indicating that the synergistic effect of low CADBH loading and an increase of rate leads to the insufficient crystallization in cooling, and that recrystallization behavior occurs in heating.

As stated in the non-isothermal melt crystallization section, a high cooling rate could severely impair the crystallization ability of PLLA/CADBH, thus, the melting heating processes of PLLA/CADBH after cooling at a relative fast rate (like 10°C/min in this study) were recorded to obtain the influences of different heating rates on PLLA/CADBH's melting behaviors. The double melting peaks are clearly visible in Fig. 9. At a given heating rate, the melting peak at low temperature shifts toward high temperature with the increasing CADBH content, which sufficiently confirms the result of the previous non-isothermal melt crystallization (Fig. 4). The PLLA containing relatively high CADBH loading crystallizes at a higher temperature during cooling. In such circumstances, the crystals formed are more perfect, resulting in a higher melting temperature during the heating step. However, on the other hand, the melting temperature of the high temperature melting peak hardly depends on CADBH content, and the melting temperature is slightly only affected by the heating rate. The melting behavior, illustrated by the low-temperature melting peak and the high-temperature melting peak, proves that the double melting peak

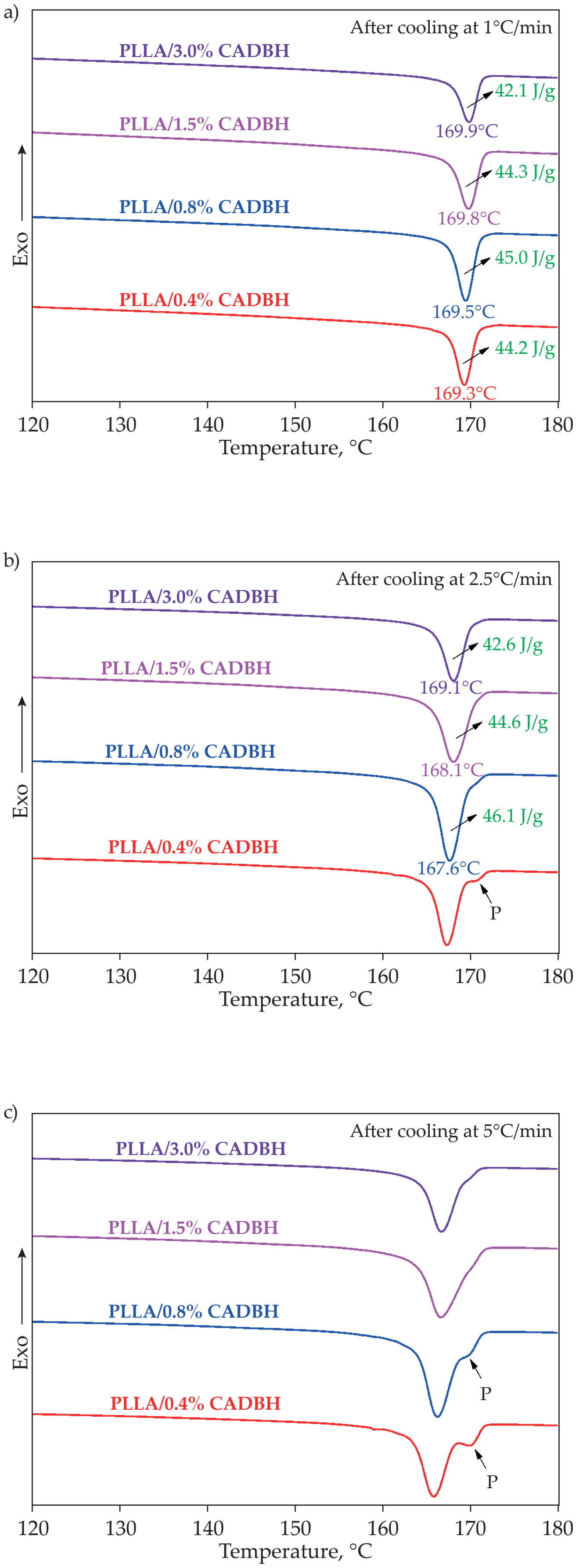

Fig. 8. PLLA/CADBH melting process at different heating rates corresponding to the rate of non-isothermal melt crystallization: a) 1°C/min, b) 2.5°C/min, c) 5°C/min

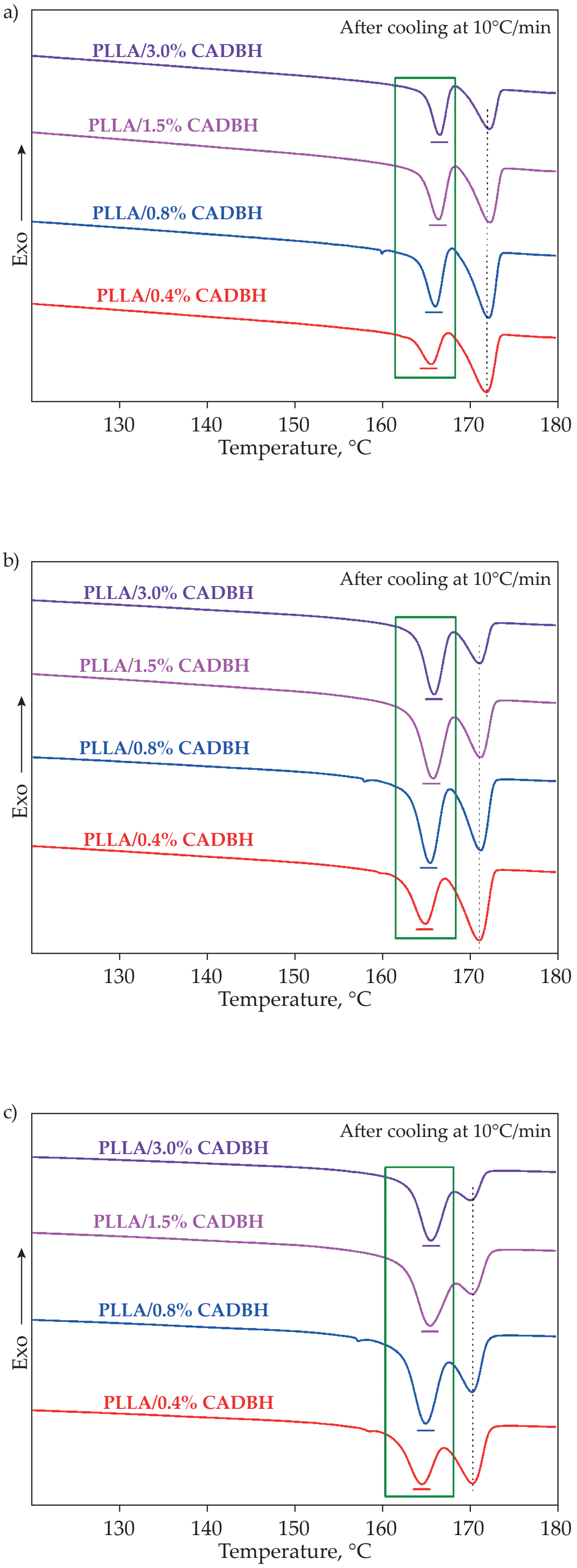

Fig. 9. PLLA/CADBH melting process at different heating rates after alloy crystallization: a) 1°C min, b) 2.5°C/min, c) 5°C/min

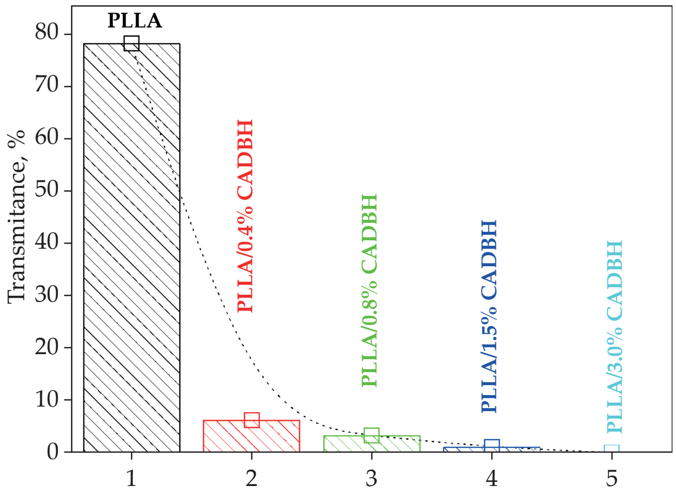

Fig. 10. PLLA transparency with or without CADBH

phenomenon is the result of the melting-recrystallization mechanism and the low-temperature melting peak is the result of melting of the primary crystals formed during cooling. High temperature melting peak can be attributed to the melting of the crystallites rapidly formed during the melting. When the heating rate is the same, the formation temperature of the reformed crystallites is close [29], leading to the same melting temperature.

Optical property

Good transparency is PLLA's a prominent feature compared with other polyesters such as polyethylene glycol terephthalate, poly(butylene succinate) and polybutylene terephthalate, but the addition of additives often impairs the excellent transparency of PLLA [30]. Thus, it is necessary to estimate CADBH's effect on PLLA's transparency. Fig, 10 shows the transparency of PLLA with or without CADBH it is truly clear that the addition of CADBH gravely damages PLLA's transparency. That is, when the CADBH loading is only 0.4 wt%, the transparency greatly decreases from 78.2% to 6.15%, when further increasing CADBH loading to 1.5 wt%, the transparency is only 1.0%, even only 3 wt% CADBH can make PLLA's transparency to be zero, and this effect of CADBH on PLLA's transparency depends on two factors including CADBH itself and an increase of PLLA's crystallinity. The addition of white CADBH affects PLLA's transparency, and the higher CADBH loading caused greater effect of CADBH on PLLA's transparency. Additionally, CADBH can enhance PLLA's crystallization capability under various conditions, and this increase of crystallinity causes light scattering to occur at the boundary between crystalline and amorphous regions, resulting in a drop in transparency.

CONCLUSIONS

In this study, a new crystallization agent CADBH was developed *via* a two-step liquid reaction, in which its effect on the physical properties of PLLA was investigated by DSC, POM, and light transmittance. CADBH effectively enhanced the crystallization kinetics of PLLA by both inducing crystallization at elevated temperatures and accelerating the crystallization rate. Furthermore, T_g analysis showed a dependence on both PLLA crystallinity and CADBH concentration. Remarkably, competitive interactions were observed between cooling rate and CADBH content in enhancing crystallization. Isothermal crystallization studies lasting more than 300 s showed incomplete coverage of the spherulite in pure PLLA by POM, indicating slow kinetics.

In contrast, PLLA/0.4% CADBH spherulites permeated the whole POM image after isothermal crystallization for 60 s, characterized by boundaryless spherulites with advanced crystal growth and interlayer interactions. PLLA/3% CADBH showed a minimum $t_{1/2}$ of 35.4 s at 115°C compared to other PLLA/CADBH. The appearance of dual melting endotherms in PLLA/CADBH with low CADBH content at moderate cooling rates (2.5°C/min and 5°C/min) directly correlated with the incomplete crystallization during cooling. The differences in the melting behavior of PLLA/CADBH at different heating rates after cooling at 10°C/min showed that the melting behavior under these circumstances depended on the heating rate and CADBH content. At the same time, the addition of CADBH seriously affected the optical transparency of PLLA – after adding only 0.4 wt% CADBH, the transparency of PLLA/0.4% CADBH was reduced by a maximum of 0.7 times compared to pure PLLA.

ACKNOWLEDGEMENTS

This study was supported by Natural Science Foundation of Chongqing Science and Technology Bureau (project number CSTB2023NSCQ-MSX1087), Science and Technology Research Program of Chongqing Municipal Education Commission (project number KJZD-K202301303, KJQN202401320), and Postgraduate Research Innovation Projects of Chongqing (project number CYS240779) and Postgraduate Research Innovation Projects of Chongqing University of Arts and Sciences (project number CUAS-GSG2024010).

Authors contribution

Y.L. – investigation, writing-review and editing; N.T. – investigation; H.Z. – data curation, writing-review and editing; Y.C. – investigation, writing-original draft; X.Z. – data curation.

Funding

This study was supported by Natural Science Foundation of Chongqing Science and Technology Bureau (project number CSTB2023NSCQ-MSX1087), Science and Technology Research Program of Chongqing Municipal Education Commission (project number KJZD-K202301303, KJQN202401320), and Postgraduate Research Innovation Projects of Chongqing (project number CYS240779) and Postgraduate Research Innovation Projects of Chongqing University of Arts and Sciences (project number CUAS-GSG2024010).

Conflict of interest

The authors declare no conflict of interest.

REFERENCES

[1] Ageyeva T., Kovacs J.G., Tabi T.: *Journal of Thermal Analysis and Calorimetry* **2021**, *147(15)*, 8199.
https://doi.org/10.1007/s10973-021-11145-y

[2] Song P., Sang L., Zheng L.C. *et al.*: *RSC Advances* **2017**, *7*, 27150.
https://doi.org/10.1039/c7ra02617j

[3] Chen X.N., Yao J., Yu J. *et al.*: *Industrial and Engineering Chemistry Research* **2022**, *61(37)*, 13921.
https://doi.org/10.1021/acs.iecr.2c02811

[4] Wang H.K., Liu X.R., Liu J.F. *et al.*: *International Journal of Biological Macromolecules* **2022**, *221*, 278.
https://doi.org/10.1016/j.ijbiomac.2022.08.121

[5] Jiang Y.P., Yan C., Wang K. *et al.*: *Materials* **2019**, *12(10)*, 1663.
https://doi.org/10.3390/ma12101663

[6] Merino D., Zych A., Athanassiou A. *et al.*: *ACS Applied Materials and Interfaces* **2022**, *14(41)*, 46920.
https://doi.org/10.1021/acsami.2c10965

[7] Hussain T., Tausif M., Ashraf M.: *Journal of Cleaner Production* **2016**, *108(Part A)*, 476.
https://doi.org/10.1016/j.jclepro.2015.05.126

[8] Liao C.G., Xiao Y.P., Chen K. *et al.*: *International Journal of Biological Macromolecules* **2022**, *221*, 773.
https://doi.org/10.1016/j.ijbiomac.2022.09.023

[9] Kalva S.N., Ali F., Velasquez C.A. *et al.*: *Polymers* **2023**, *15(11)*, 2572.
https://doi.org/10.3390/polym15112572

[10] Zhang Q.F., Cai H.Z., Zhang A.D. *et al.*: *Polymers* **2018**, *10(9)*, 932.
https://doi.org/10.3390/polym10090932

[11] Finkenstadt V.L., Tisserat B.: Industrial Crops and Products **2010**, *31(2)*, 316.
https://doi.org/10.1016/j.indcrop.2009.11.012

[12] Song P., Sang L., Zheng L.C. *et al.*: *RSC Advances* **2017**, *7*, 27150.
https://doi.org/10.1039/C7RA02617J

[13] Pan P.J., Yang J.J., Shan G.R. *et al.*: *Macromolecular Materials and Engineering* **2012**, *297(7)*, 670.
https://doi.org/10.1002/mame.201100266

[14] He Z.J., Shao H.F., Zhang N.N. *et al.*: *Journal of Polymer Science* **2023**, *61(1)*, 67.
https://doi.org/10.1002/pol.20220295

[15] Li Y., Han C.Y., Yu Y.C. *et al.*: *Journal of Thermal Analysis and Calorimetry* **2019**, *135(4)*, 2049.
https://doi.org/10.1007/s10973-018-7365-x

[16] Wang S.S., Han C.Y., Bian J.J. *et al.*: *Polymer International* **2011**, *60(2)*, 284.
https://doi.org/10.1002/pi.2947

[17] Cai Y.H., Zhao L.S.: *Materials Research Express* **2017**, *4*, 035305.
https://doi.org/10.1088/2053-1591/aa6362

[18] Liang J.Z., Zhou L., Tang C.Y. *et al.*: *Composites Part B: Engineering* **2013**, *45(1)*, 1646.
https://doi.org/10.1016/j.compositesb.2012.09.086

[19] Yang J.N., Nie S.B., Qiao Y.H. *et al.*: *Journal of Polymers and the Environment* **2019**, *27(12)*, 2739.
https://doi.org/10.1007/s10924-019-01557-1

[20] Niu D.Y., Shen T.F., Xu P.W. *et al.*: *International Journal of Biological Macromolecules* **2023**, *234*, 123584.
https://doi.org/10.1016/j.ijbiomac.2023.123584

[21] Gui Z.Y., Lu C., Cheng S.J.: *Polymer Testing* **2013**, *32(1)*, 15.
https://doi.org/10.1016/j.polymertesting.2012.08.011

[22] Wang L., Wang Y.N., Huang Z.G. *et al.*: *Materials and Design* **2015**, *66(Part A)*, 7.
https://doi.org/10.1016/j.matdes.2014.10.011

[23] Tan J., Cui L.N., Qin Z.X. *et al.*: *CrystEngComm* **2025**, *27(12)*, 1722.
https://doi.org/10.1039/d4ce01249f

[24] Huang H., Lv Y., Zhao L.S. *et al.*: *Materials Science-Poland* **2024**, *42(2)*, 100.
https://doi.org/10.2478/msp-2024-0024

[25] Zhao L.S., Qiao J., Shan X.L. *et al.*: *Materiale Plastice* **2021**, *58(1)*, 57.
https://doi.org/10.37358/Mat.Plast.1964

[26] Zhao L.S., Liu X.H., Cai Y.H. *et al.*: *Journal of Thermoplastic Composite Materials* **2023**, *36(1)*, 218.
https://doi.org/10.1177/08927057211001921

[27] Huang H., Zhang Y.H., Zhao L.S. *et al.*: *Materiale Plastice* **2020**, *57(3)*, 28.
https://doi.org/10.37358/Mat.Plast.1964

[28] Zhang H.C., Huang J.T., Yang L. *et al.*: *RSC Advances* **2015**, *5(6)*, 4639.
https://doi.org/10.1039/C4RA14538K

[29] Xin C.Z., Zhang H., Wang Y.W. *et al.*: *Plastics Science and Technology* **2017**, *45(1)*, 74.
https://doi.org/10.15925/j.cnki.issn1005-3360.2017.01.012

[30] Zhao L.S., Cai Y.H., Liu H.L. *et al.*: *Polymer-Plastics Technology and Materials* **2020**, *59(2)*, 117.
https://doi.org/10.1080/25740881.2019.1625386

Received 13 IV 2025.
Accepted 29 IV 2025.